A SIMPLIFIED METHOD FOR THE PHOTOELASTIC
DETERMINATION OF STRESS CONCENTRATION FACTORS
IN A TENSILE STRESS FIELD

by

Ronald B. Carr

Thesis submitted to the Graduate Faculty of the
Virginia Polytechnic Institute
in candidacy for the degree of

MASTER OF SCIENCE

in

ENGINEERING MECHANICS

May, 1962
Blacksburg, Virginia

I. TABLE OF CONTENTS

4

II. LIST OF FIGURES AND TABLES

III. INTRODUCTION

In the field of stress analysis, there are many problems that have been solved mathematically based upon the assumption that a state of plane stress exists throughout the body. To verify the theory involved, each problem must be experimentally confirmed. To facilitate this experimental work, a method of loading a circular disk such as to create a uniaxial tension field, was investigated for the examination of stress concentration factors.

A major portion of this thesis deals with the photoelastic investigation of the loading of a circular disk. As an example of the use of this disk, a series of slots with rounded ends were examined with regard to the value of the stress concentration factors as the slot was oriented at different angles with respect to the direction of the tension field.

The standard photoelastic method of photographing the fringe pattern to determine the value of the maximum stress at the edge of the slot was not used. Instead a method was developed for determining the value of the stress concentration factor which required only the recording of the load applied to the plate when each fringe appeared at the edge of the slot. A portion of this paper was thus devoted to the difficulties in using this method and the technique of eliminating or minimizing the errors.

IV. THE REVIEW OF LITERATURE

Since the original conception of the photoelastic effect by Sir David Brewster in 1816[8], there have been numerous applications to all types of plane stress problems and even to three dimensional stress analysis.[1] [4] [5]

The problem of a circular disk loaded in compression at diameterically opposed points has been solved mathematically by H. Hertz[11] and has been investigated experimentally by M. M. Frocht.[6] A complete investigation of the stress concentration factor for various slots with their major axes perpendicular to the field of tension in a plate of finite width was done by M. M. Frocht and M. M. Leven in 1950.[4]

One of the most complete collections of stress concentration factors was compiled by R. E. Peterson in 1953.[10] In this collection he presents both the experimental results of many contributers and also the stress concentration factors that have been solved for mathematically. Much of the mathematical work involving the study of notches and grooves has been considered by Neuber.[9]

V. THE INVESTIGATION

5.1 OBJECTIVES OF THE INVESTIGATION

The investigation was considered in two parts.

5.1.1 Part I of the investigation consisted of the development of appropriate equipment and techniques for use in a simplified method for obtaining the solution to classes of problems described in Article 5.1.2. A method for loading a circular disk in tension was developed which would provide:

a.   approximately uniform simple tension field over the majority of the disk and,

b. a means of varying the direction of tension relative to the stress raisers in the tensile field.

The use of the method of recording the loads at which each fringe appeared on the edge of the stress concentration to determine the value of the stress concentration factor should yield satisfactory results. For a complete discussion of the method to be employed see Article 5.3.

5.1.2 Part II of the investigation dealt with the photoelastic determination of stress concentration factors for rectangular slots with semi-circular ends inclined at various angles to a stress field of approximately uniform simple tension as described in Article 5.1.1. The results in using a circular disk were to be compared with the results of a slot in a rectangular plate.

PART I. DEVELOPMENT OF EQUIPMENT AND TECHNIQUES

5.2 METHODS OF LOADING THE CIRCULAR DISK

Before achieving the first objective of this investigation, four methods of loading a circular disk to create a uniaxial tension field were investigated.

5.2.1 The first method attempted consisted of trying to load through a circle of holes drilled around the perimeter of the disk.

The material, CR-39, was machined into a six inch diameter disk. Two sets of loading plates were constructed of one-eighth inch thick steel, as shown in FIGURE 1. Each of the six holes were drilled through the four plates at the same time. To facilitate the accurate alignment of the holes in the steel plates with the holes in the disk, one of the steel plates was used as a guide. The model was marked by tapping the drill against the model through each hole in the steel plate. Then using these marks, the holes were drilled in the disk.

Two different attempts were made to use this loading device. The first consisted of placing bolts through the steel plates and disk, as shown in FIGURE 1, without tightening the bolts. Upon placing the disk in the plane of the circularly polarized light of the polariscope and loading the model through points A and B, as shown in FIGURE 1. It was evident by observation of the fringe pattern that the plate was not under uniform tension, as fringes originated from bolts one, four, and nine, instead of one uniform fringe over the middle section of the plate. Therefore, this attempt was abandoned as being unsatisfactory, because the
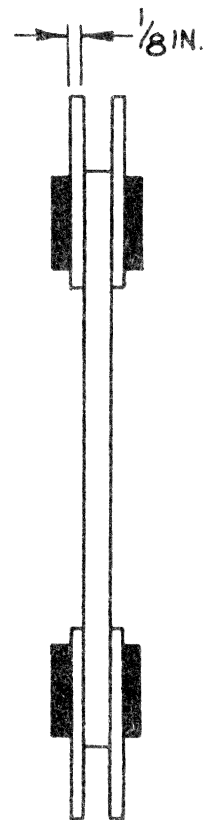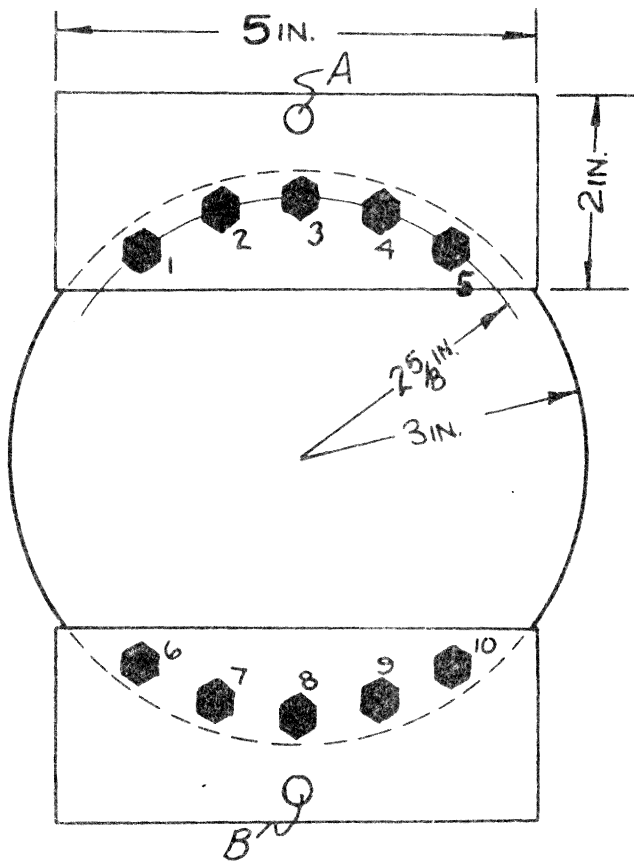
5 IN.

A

1 2 3 4 5

2 IN.

2⁵⁄₈ IN.

3 IN.

6 7 8 9 10

B

¹⁄₈ IN.
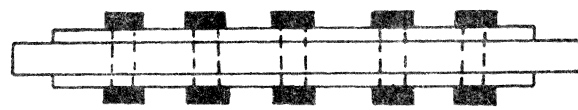
FIGURE 1- LOADING METHOD 5.2.1

bolt alignment was too critical to produce a uniform tension field.

With the same steel plates and the same circle of holes, the disk was then clamped by tightening the ten bolts. The attempt here was to distribute the load by friction through the enclosed portion of the plate. This method was also unsatisfactory as some of the bolts were still in contact with the model and created fringes that extended down into the plane of the plate.

5.2.2 The same steel plates used in investigation of Method 5.2.1 were then modified by drilling a line of holes , as shown in FIGURE 2. Care was again taken in alignment of these holes with a series of holes drilled in the model. The same method to align the holes used in Method 5.2.1, was repeated for Method 5.2.2. This method was deemed unsatisfactory by inspection of the fringe pattern, for the same reason as Method 5.2.1.

5.2.3 After the realization that the alignment of the holes was too critical to rely on reproducibility of the uniform stress field, the disk was then clamped, as shown in FIGURE 3. A new set of steel clamping plates were machined of one-fourth inch material to achieve a rigid clamp. Here the attempt was to eliminate all bolt contact with the disk.

The clamping device consisted of the two sets of steel plates shown in FIGURE 3 and also two sets of plastic backing plates which the steel plates clamped onto as well as the model. The entire loading was done through friction across the surface shown crosshatched in FIGURE 3.

FIGURE 2 - LOADING METHOD 5.2.2

FIGURE 3 - LOADING METHOD 5.2.3

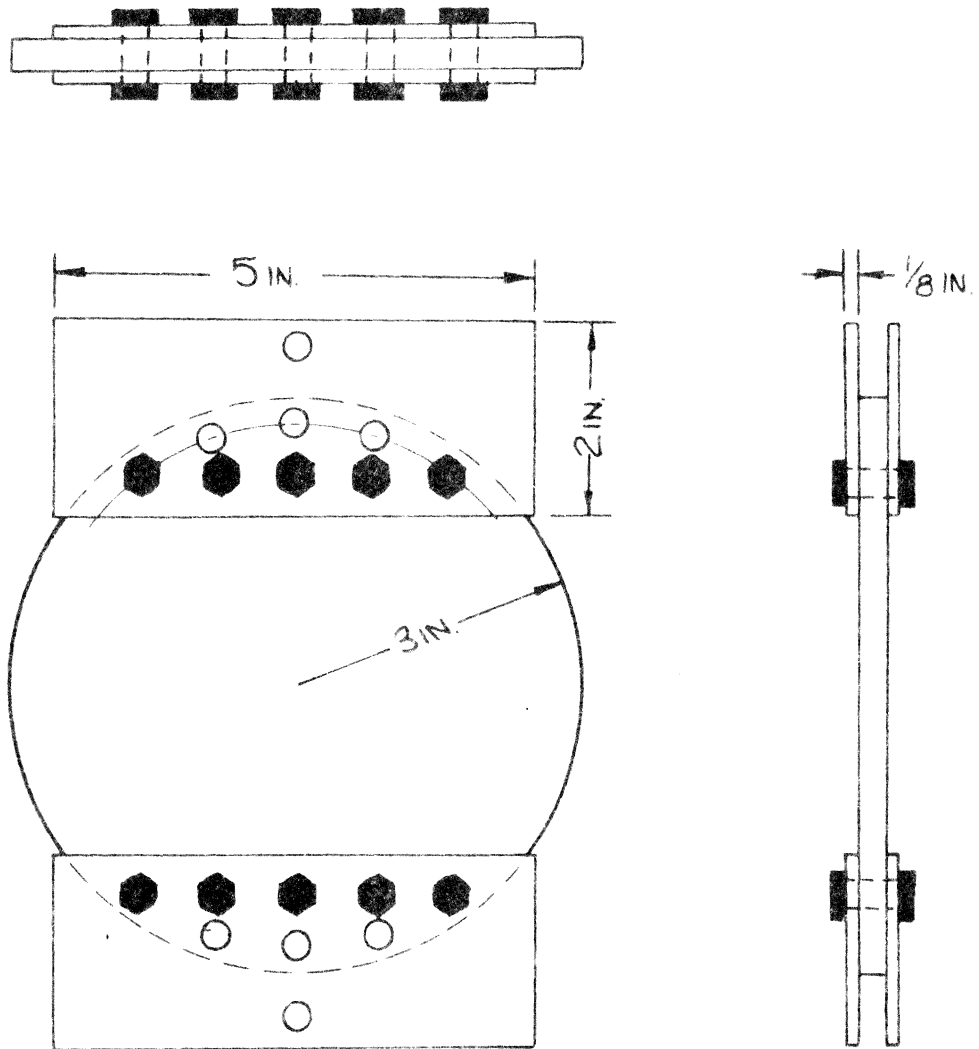///// FRICTIONAL SURFACE
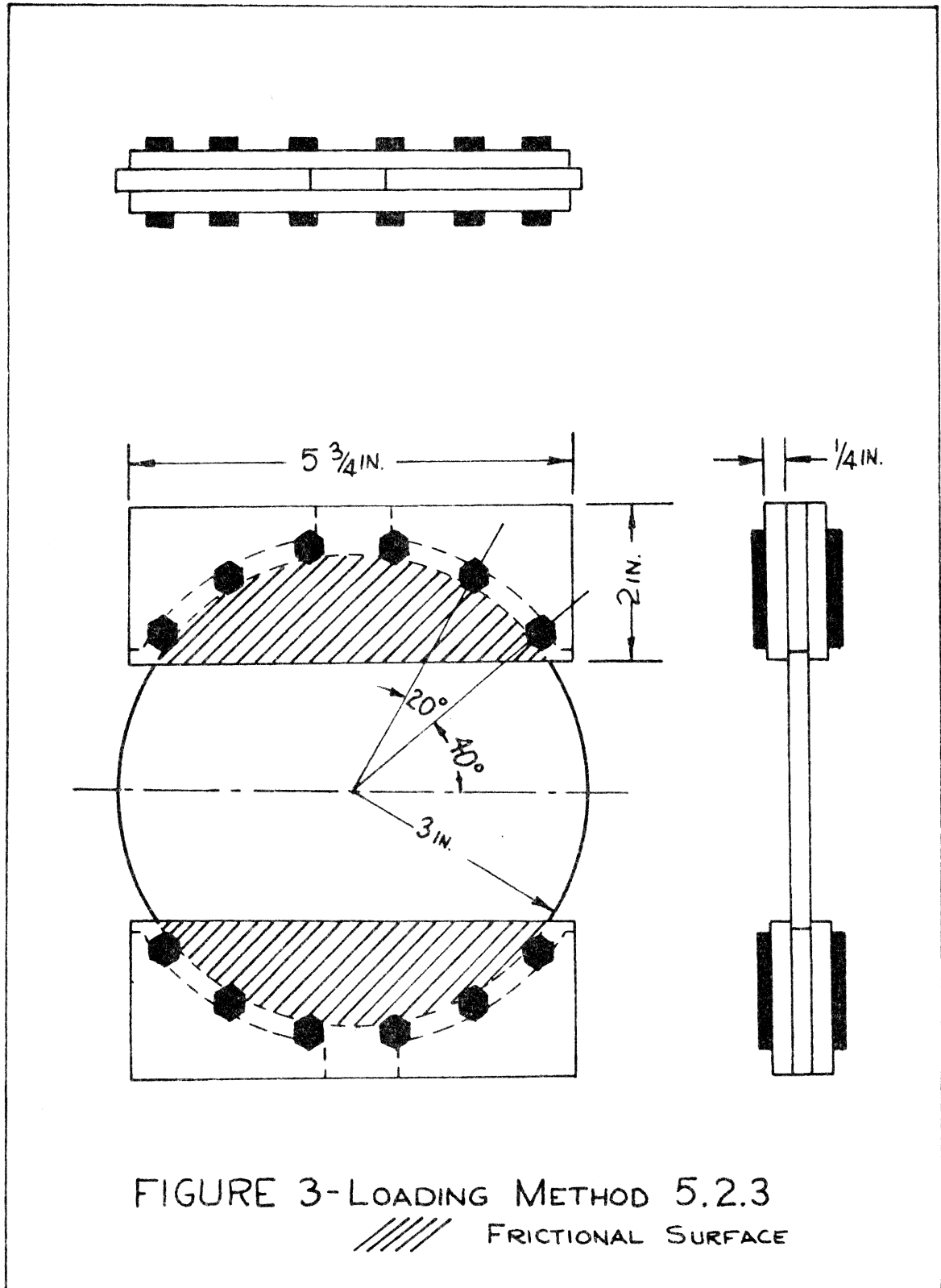
With this arrangement the fringe pattern, as seen in the circular polariscope, appeared more nearly uniform than those of Methods 5.2.1 and 5.2.2. However, where the steel clamp came into contact with the disk, there were fringes extending into the field of the disk, from the clamping action of the steel plates. Because this localized effect extended about one-half inch into the plane of the disk from each clamp, this method was not used.

5.2.4 The same two sets of steel clamping plates were used for this method, as for Method 5.2.3, with the addition of two sets of plastic liners, as shown in FIGURE 4. These plastic liners were used as a means of distributing the clamping load away from the relatively rigid edge of the steel plates and thus eliminate the local affect that was undesirable in Method 5.2.3.

In FIGURE 5, the position of the additional liner is shown. The plastic liner extended farther into the plane of the disk than the steel plates to aid in distributing the load away from the edge of the steel plate.

Upon loading the disk through points A and B, as shown in FIGURE 4, it was evident that a large portion of the disk was subject to uniaxial tension. A single fringe formed over the middle section of the disk and the isoclinic pattern verified the symmetry of loading, as shown in FIGURE 6.

It was still observable that portions of the edge of the model were not under uniform tension, but to try to put this section of the plate under uniform tension would have meant enclosing more of the disk and

FIGURE 4 - LOADING METHOD 5.2.4

///// FRICTIONAL SURFACE

15
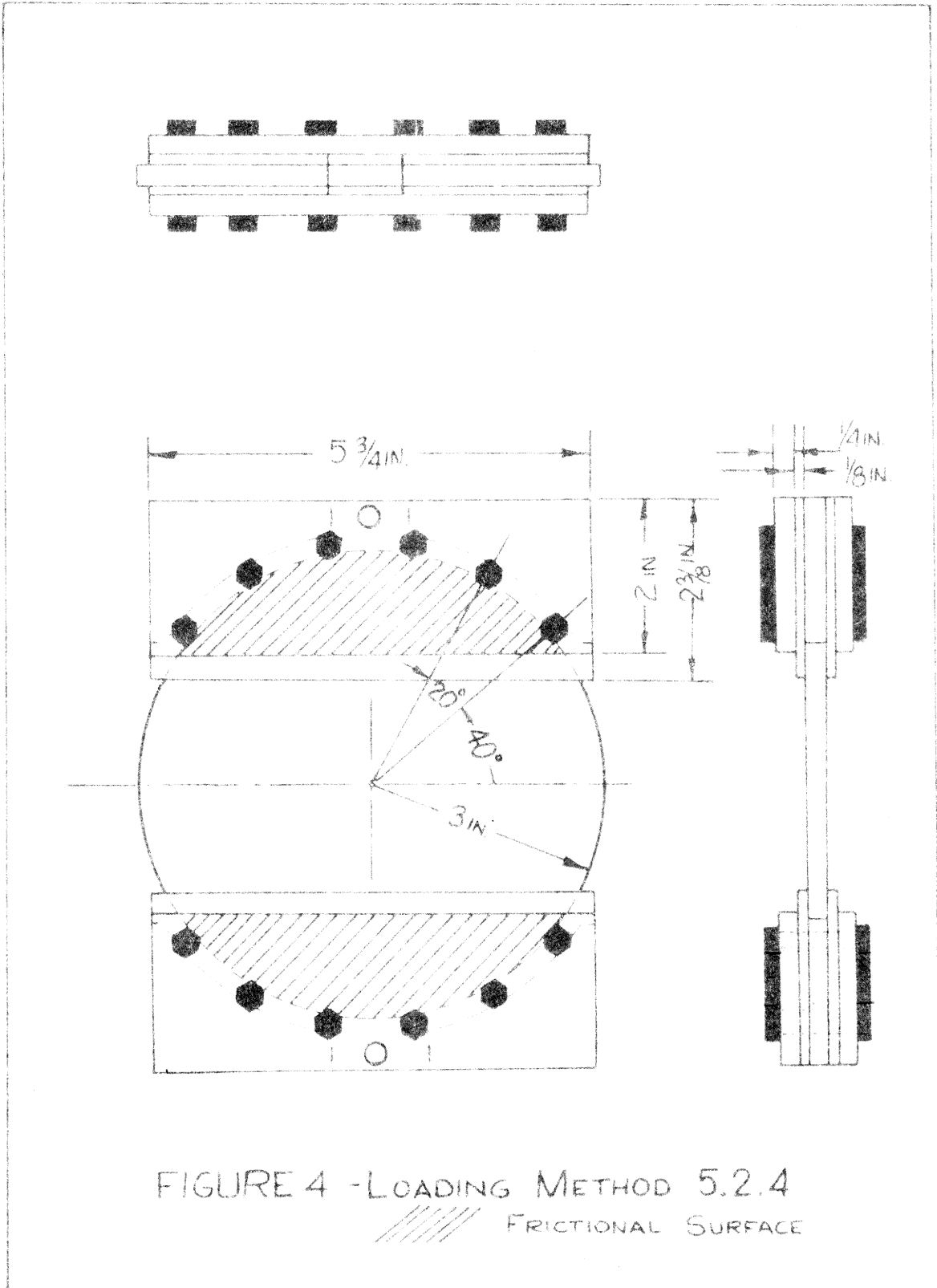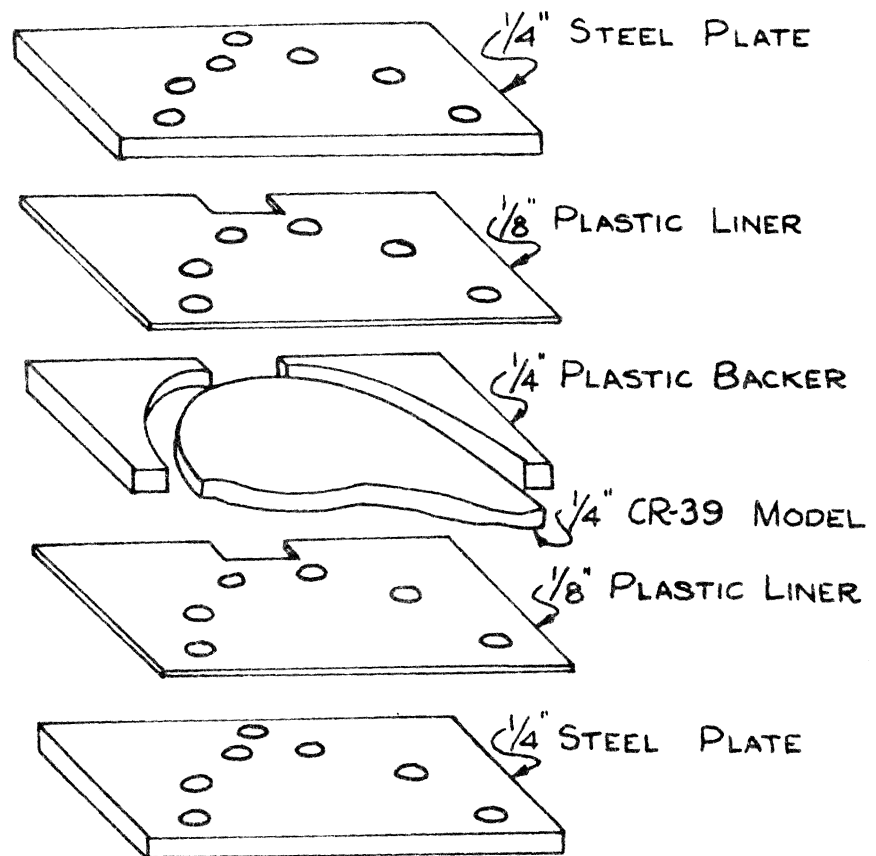
FIGURE 5- EXPLODED LOADING
FIXTURE 5.2.4

FIGURE 6 - FRINGE AND ISOCLINIC PATTERN FOR THE DISK
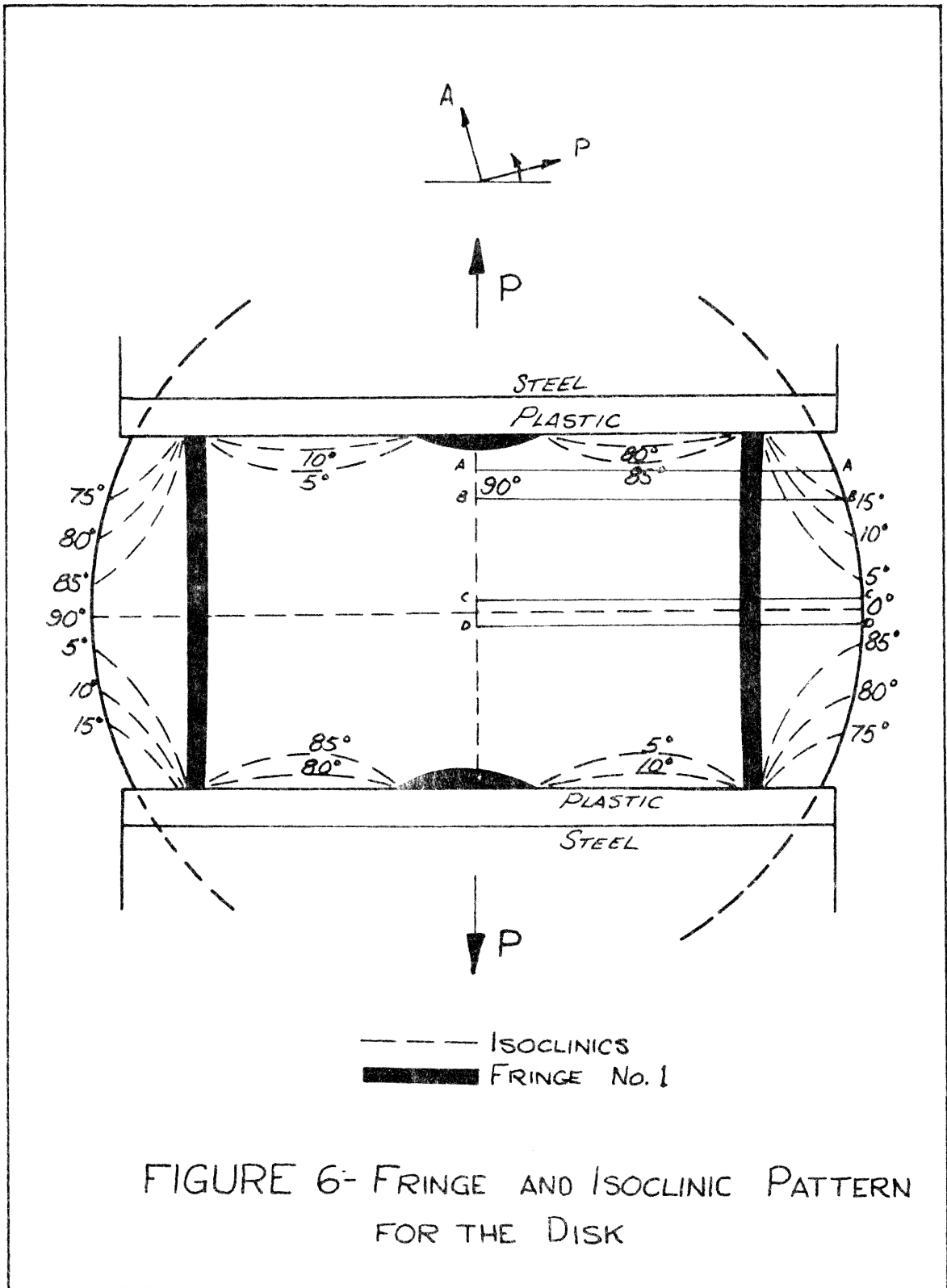
this would have decreased the size of the uniform field more than the additional edge area would increase the field size. From this standpoint, Method 5.2.4 was considered acceptable. This method of loading the disk was used throughout the remainder of the investigation.

5. 3 CALCULATION OF STRESS CONCENTRATION FACTORS

The definition of stress concentration factor that was used in this thesis was:

$$\sigma_C = K_t \sigma_{net} \qquad (5.3.1)$$

where σ_C corresponds to the maximum value of the stress next to the slot, σ_{net} is the applied load divided by the critical cross section of the member. This corresponds to the definition used by M. M. Frocht and M. M. Leven in their investigation of stress concentration factors for slots. A discussion of σ_{net} for the slots at an angle with the direction of the uniaxial tension field is included in Appendix 11.1.

From the above definition of stress concentration factor and basic photoelastic concepts, a method for calculating the stress concentration factor for any model was developed. The main advantage of this method is that it enables one to determine a stress concentration factor without investigating the entire model and requires only the recording of certain loading information as each fringe forms on the edge of the slot.

The material fringe value, which is a constant for any local area of a material, can be calculated by knowing the values of the principal

stresses, corresponding fringe order, and material thickness.[8] The material fringe value is given by Neumann's Equation as:

$$f = \frac{(\sigma_1 - \sigma_2)h}{n} , \quad \frac{lb.}{in. \ x \ order} \qquad (5.3.2)$$

where: f = Material fringe value,

            h = Material thickness,

            n = Fringe order,

        σ_1 , σ_2 = Principal stresses.

One common method for determining the material fringe value is by the use of a simple tension member. The formula for the material fringe value thus becomes:

$$f = \frac{P_C}{(W_C)(n_C)} \qquad (5.3.3)$$

where: P_C = The applied tensile load,

            W_C = Width of the member,

            n_C = Fringe number.

as shown on FIGURE 7-a.

Instead of using a tension member to determine the material fringe value, consider using a member with a stress concentration in it, as shown in FIGURE 7-b. The stress at point C is:

from (5.3.1): $\sigma = K_t \sigma_{net}$

Therefore, using this relationship for calculating the material
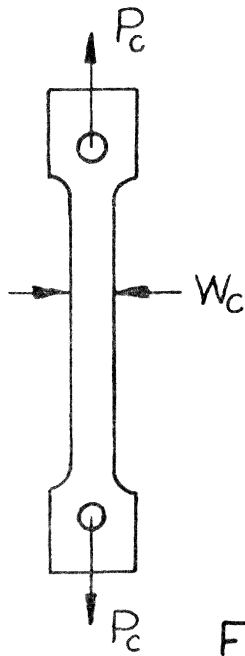
FIGURE 7-a
TENSION MODEL
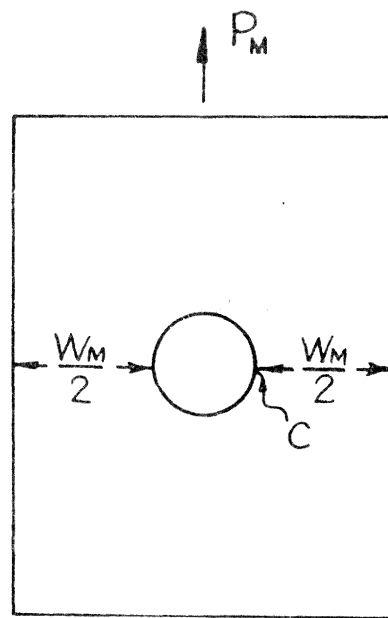
FIGURE 7-b
MODEL WITH HOLE

fringe value, where the orthogonal normal stress in the free surface is zero:

from (5.3.2):
$$f = \frac{(K_t)\,(\sigma net)(h)}{(n)}$$

or,
$$f = \frac{(K_t)(P_m)}{(W_m)(n_m)} \qquad (5.3.4)$$

since the material fringe value is a constant:

from (5.3.3) and (5.3.4):
$$f = \frac{(P_t)}{(W_t)(n_t)} = \frac{(K_t)(P_m)}{(W_m)(n_m)} \qquad (5.3.5)$$

and, solving for K_t:
$$K_t = \frac{W_m\,(P_t/n_t)}{W_t\,(P_m/n_m)} \qquad (5.3.6)$$

where:

W_m = Net width of the model,

W_t = Width of the tension specimen,

(P_t/n_t) = Slope of the applied load-fringe number curve, for the tension specimen,

(P_m/n_m) = Slope of the applied load-fringe number curve for the model.

Using the above relation to determine the value of the stress concentration factor only requires the recording of the load on the model, P_m, as each fringe, n_m, appears at the edge of the hole. The other quantities for any one investigation remain constant and were determined from a simple tension test. It should be noted that this method can only

be applied to points at which a uniaxial stress state exists.

5. 4 TECHNIQUE OF OBSERVATION

The procedure for determining the stress concentration factor derived in the preceding section was employed in the laboratory. Although the method was simple enough in theory, the main weakness in actual practice was the human inability to observe exactly when the fringe had formed on the edge of the hole. An observer must develop an accurate technique in order to record the load exactly as each fringe appeared at the edge of the hole. There are several precautions which were an aid in observing the formation of the fringe.

5. 4. 1 A bright monochromatic light source, such as a mercury vapor lamp, makes the fringes sharper than the incandescent lamp.

5. 4. 2 A magnifying glass was used to enlarge the edge of the slot. Care had to be taken in using the magnifying glass, as any distortion tended to increase the difficulty in observing the slot, which would offset the advantage of enlargement.

5. 4. 3 A stress free edge makes the observance of the formation of each fringe easier. It should be noted, however, that this was not necessary for the analysis of the stress concentration factors.

5. 4. 4 By the performance of several reapplications of each loading cycle, any obvious errors were discarded.

5.4.5 The formation of a fringe on the edge of a large slot was much easier to observe than on a small slot. Thus large models should be used for the analysis of various stress concentration factors.

5.4.6 The greatest aid for observing the formation of the fringe was found to be the experience in observation obtained by running many preliminary tests, and acquiring the technique required for good accuracy.

5.5 TECHNIQUE OF MODEL MAKING

All models used in this investigation were made of one-fourth inch thick CR-39. Since the outer edge of the disk was not of interest, as far as stress analysis, it was not necessary to have a stress free outer edge.

The disk was cut within a half-inch of its finished dimension by a hand operated coping saw. The rough disk was then attached by the model making tape to a six inch diameter template. The Chapman Model Making Kit was then used to mill the model down to 0.007 inches of the finished size. The large template guide plug was then removed and replaced with the small template guide plug. Using light sweeping strokes, the model was milled down to its finished dimension.

From preliminary work, it was found that a hole free from edge stresses made the observation of the fringe formation easier. Therefore, care was taken in machining all slots. First a hole was drilled in the center of the model by using the one-fourth inch plastic drill provided with the Chapman Model Making Kit. This drilling was performed under

water using light drill pressure and intermittent cutting to allow the water to keep the plastic cool. All subsequent machining was done on a milling machine by lightly end milling without the use of a coolant.

5.6 MODEL MATERIAL

For preliminary investigations, the plate of CR-39 was three years old. After several tests were performed, it was determined that the material fringe value varied considerably from the edge of the plate to the center, as shown in FIGURE 8. Since the material fringe value was not constant in the local area of one model, it was impossible to use the aged material. A new plate of CR-39 was procured, which exhibited very uniform material fringe values.

5.7 LIGHT SOURCES

For the preliminary work, a 100 watt incandescent light source was used in conjunction with a 4800 $\overset{o}{A}$ filter. This produced a uniform intensity light field, but the fringes were no distinct. The use of a mercury-vapor lamp did not produce a uniform intensity light field, but yielded a bright oval field three and one-fourth inches high and two and one-half inches wide.

From the standpoint of a complete photoelastic analysis, a non-uniform light field would be undesirable, but the mercury-vapor lamp produced sharper fringes. Since this investigation only required the observance of one part of the model, the mercury-vapor lamp was used.

150

120

Pounds

90

60

30

KEY:
▣ MODEL TAKEN FROM CENTER
  OF PLATE, $f=45.3$ lb./fringe/in.
○ MODEL TAKEN FROM EDGE
  OF PLATE, $f=38.8$ lb./fringe/in.

0

0   1   2   3   4

n - FRINGE ORDER
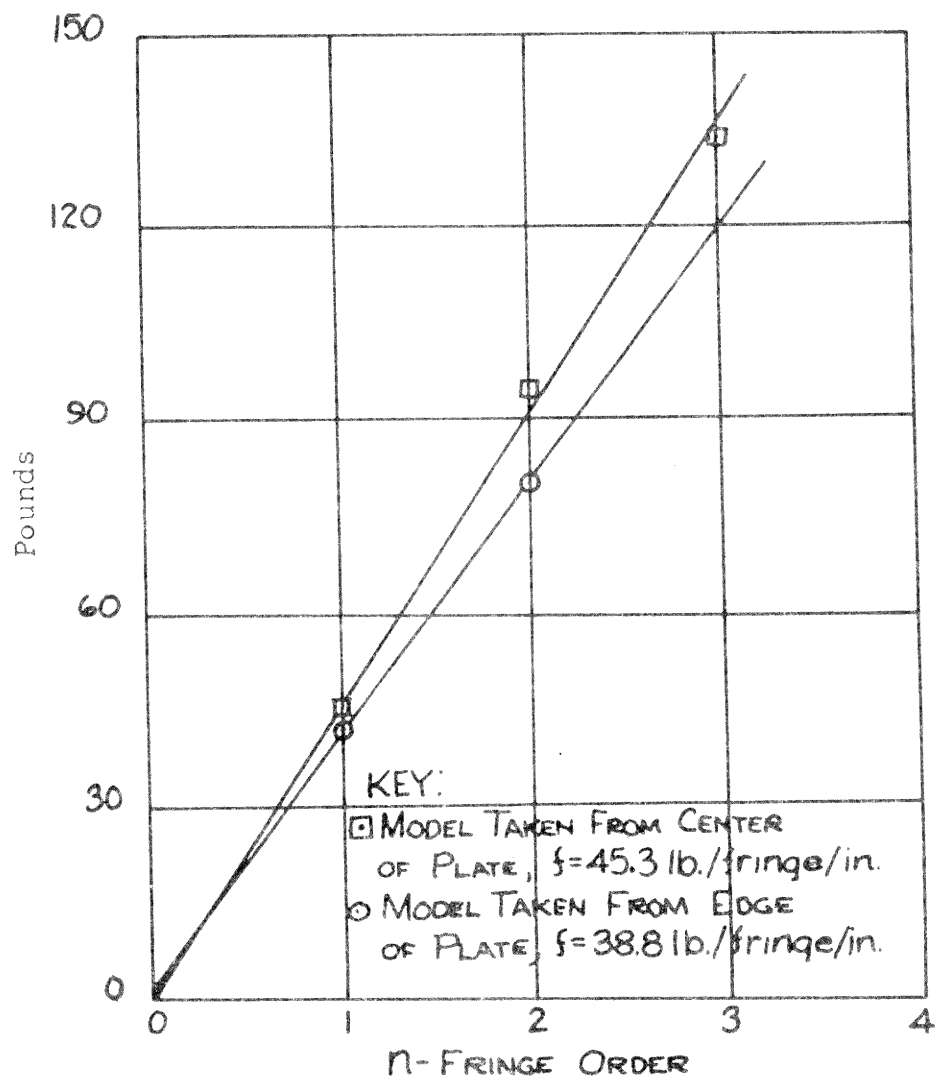
FIGURE 8 - CALIBRATION CURVE VARIATION FOR
THE THREE YEAR OLD CR-39

5. 8 POLARISCOPE

The General Radio Polariscope, Type No. 1534 located in the Engineering Mechanics Laboratory at Virginia Polytechnic Institute, was used for all tests. The polariscope and loading frame are shown in FIGURE 9.
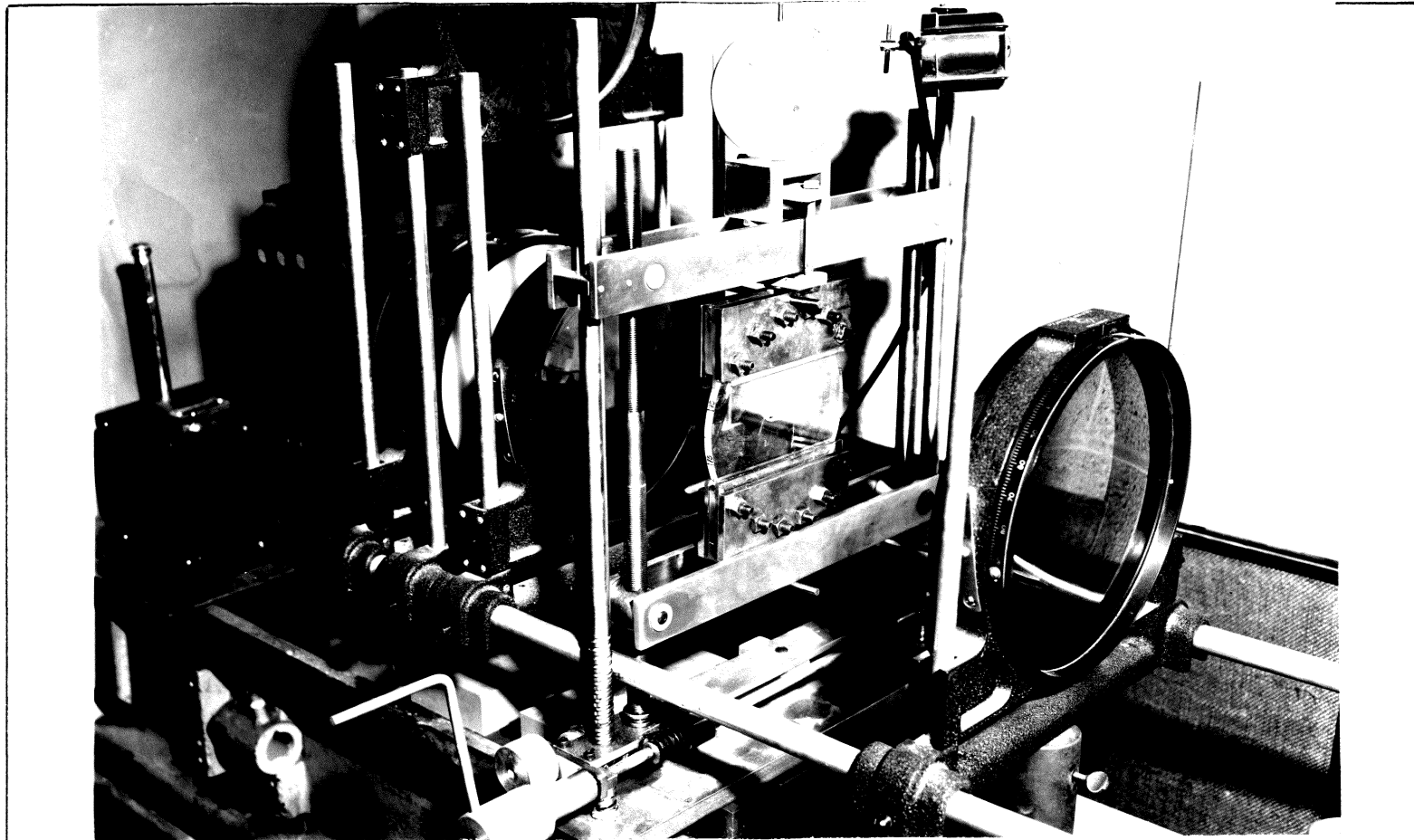
KEY:
1. Mercury Vapor Lamp
2. 4800 Å Filter (Not used)
3. Diffuser
4. Polarizer and Quarter Wave Plate
5. Load Indicator
6. Model and Loading Method 5. 2. 4
7. Analyzer and Quarter Wave Plate
8. Loading Frame

FIGURE 9 - POLARISCOPE AND LOADING FRAME

PART II. THE PROBLEM INVESTIGATED

5.9 DESCRIPTION

As an example of the use of the circular disk loaded in tension
as prescribed by Method 5.2.4, a series of slots, rectangular holes
with semi-circular ends, were investigated. Referring to FIGURE 10, the
series of slots had a t/r ratio of one, two, and four, and two such series
were investigated, the first with and r of one-eighth inch and the second
with an r of one-fourth inch. Each slot was rotated through 90° in 15°
increments, with respect to the direction of the uniform tension field.
For each increment of rotation, the load was increased while the edge
of the hole nearest the edge of the plate was observed. * As each fringe
crossed the edge of the hole, the corresponding load was recorded.

Since the slots with an r of one-eighth inch were small and thus
difficult to observe, three or more loading cycles were performed. Each
loading cycle consisted of recording data as the load was being applied,
and again as the load was being released. For the slots with an r of one-
fourth inch, two or three loading cycles were performed. depending on the
consistency of the data.

The first investigation for each slot with the major axis of the
slot perpendicular to the field of tension has been solved photoelastically
by M. M. Frocht and M. M. Leven[4] and the results are presented in

---

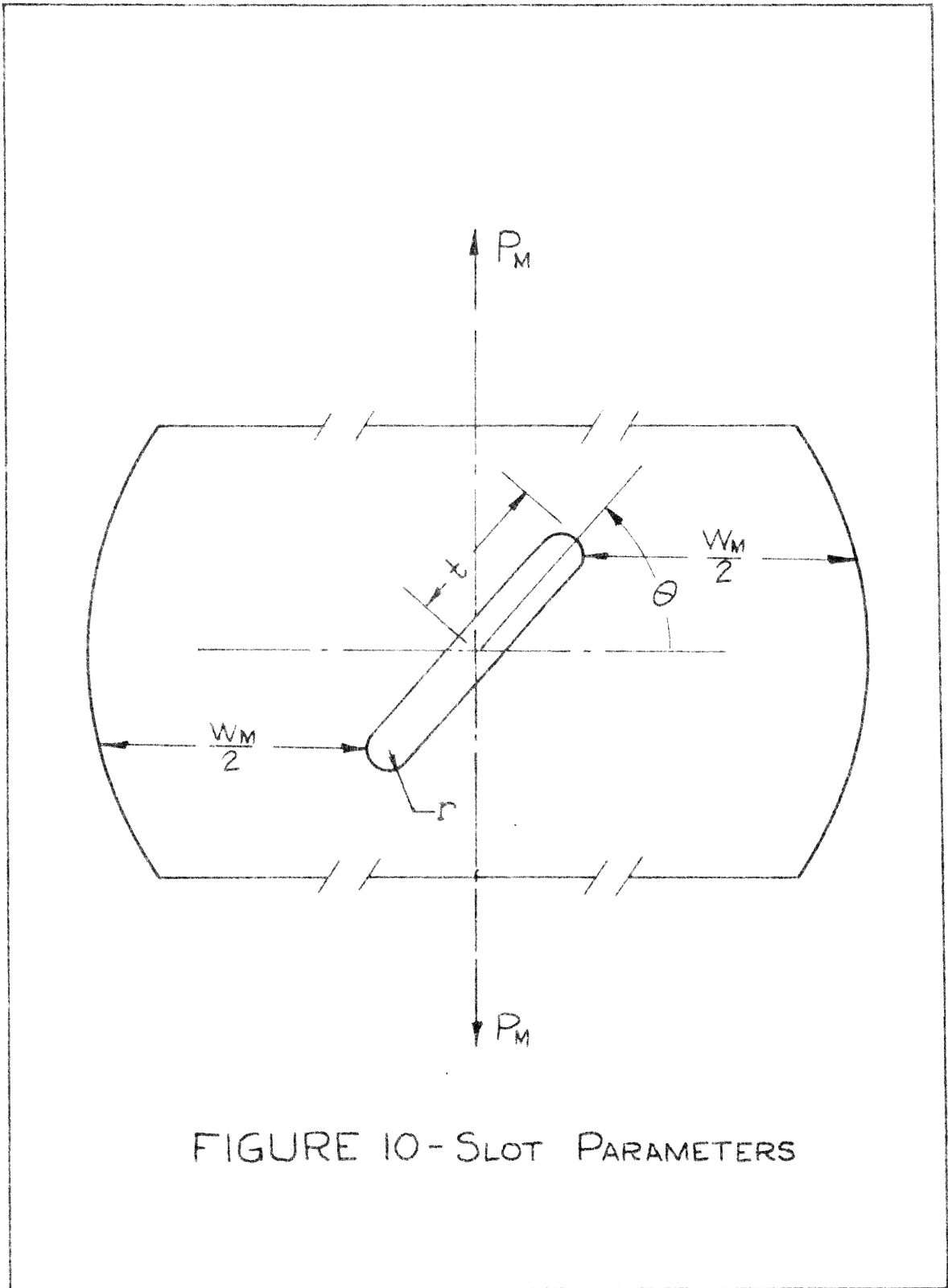* The maximum stress always occurs at this point. [9]

FIGURE 10 - SLOT PARAMETERS

"Stress Concentration Design Factors" by R. E. Peterson. This problem was used as a verification of the method.

5. 10 RESULTS

The results obtained in terms of the three objectives were as follows:

5. 10. 1 The investigation of the fringe and isoclinic pattern of the disk, as loaded by Method 5. 2. 4, gave the stress distributions, as shown in FIGURE 11. These results were calculated by the shear difference method, as given in Appendix 11. 2

5. 10. 2 For a direct comparison of the method employed to determine the stress concentration factors, three of the disks were machined to have straight edges and the results of these three tests are presented in Appendix 11. 3.

5. 10. 3 On FIGURES 12 through 15 the values of the stress concentration factors for the slots are shown as calculated by the Method of Article 5. 3, (see Appendix 11. 6 for a sample calculation). The known values for the stress concentration factors of a slot perpendicular to the direction of the field of tension were represented as solid characters for purposes of comparison. For the slots parallel to the field of tension, θ equal to ninety degrees, the values for the stress concentration factors for a fillet were represented as solid characters. The reason for the slot parallel to the stress field being compared to a fillet is discussed in Appendix 11. 4.

FIGURE 11- STRESS DISTRIBUTION FOR THE LOADED DISK WITHOUT A SLOT

KEY:
□ VALUES OBTAINED FROM DISK, t/r=1
■ RECTANGULAR PLATE[10], t/r=1
⊙ VALUES OBTAINED FROM DISK, t/r=2
● RECTANGULAR PLATE[10], t/r=2
▲ FILLET[10]
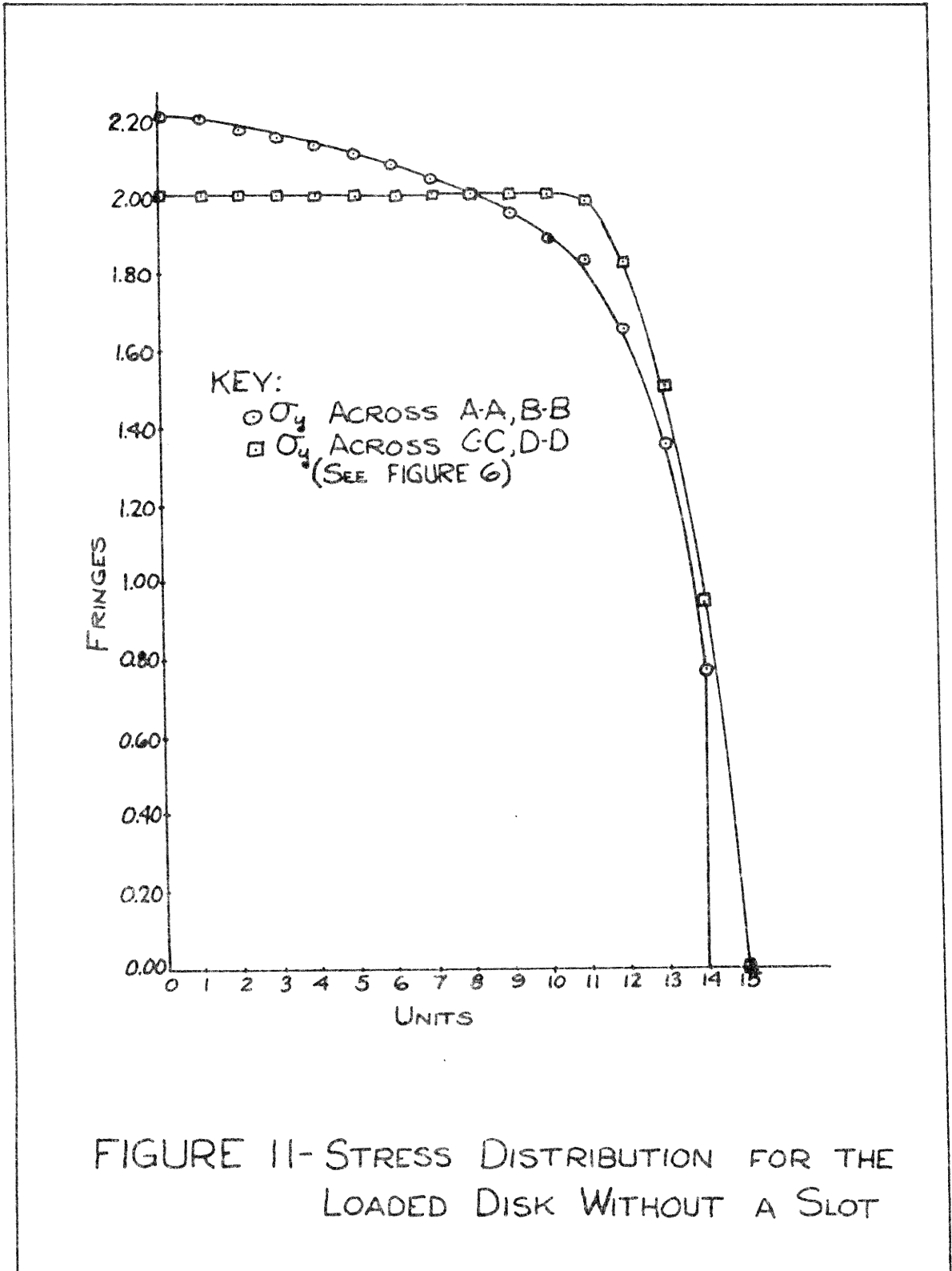
FIGURE 12 - STRESS CONCENTRATION FACTOR FOR t/r=1 AND t/r=2, r=1/8 INCH VERSUS θ

FIGURE 13-STRESS CONCENTRATION FACTOR FOR
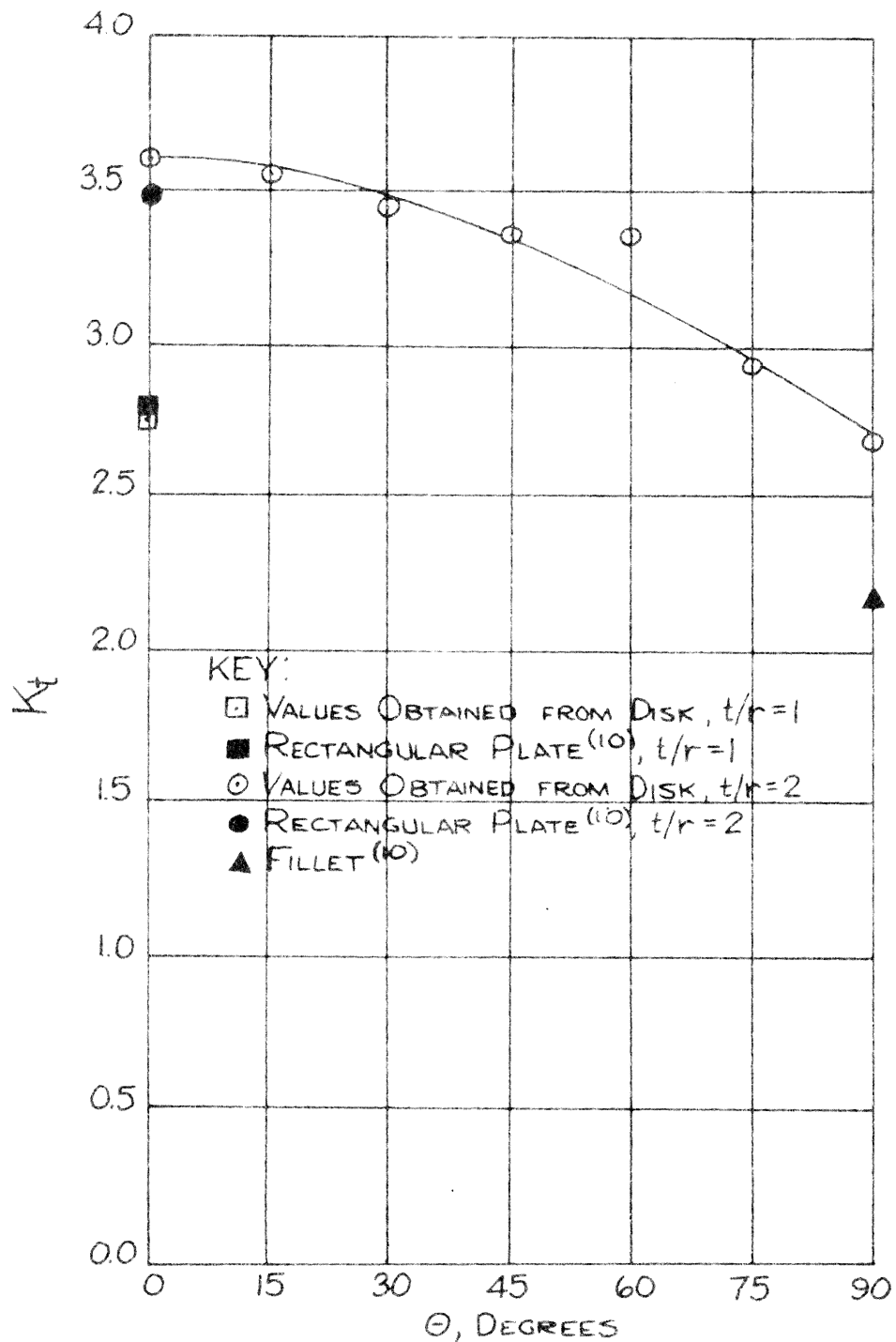$t/r=4$, $r=\frac{1}{8}$ INCH VERSUS Θ

FIGURE 14- STRESS CONCENTRATION FACTOR FOR $t/r=1$, AND $t/r=2$, $r = \frac{1}{4}$ INCH VERSUS θ

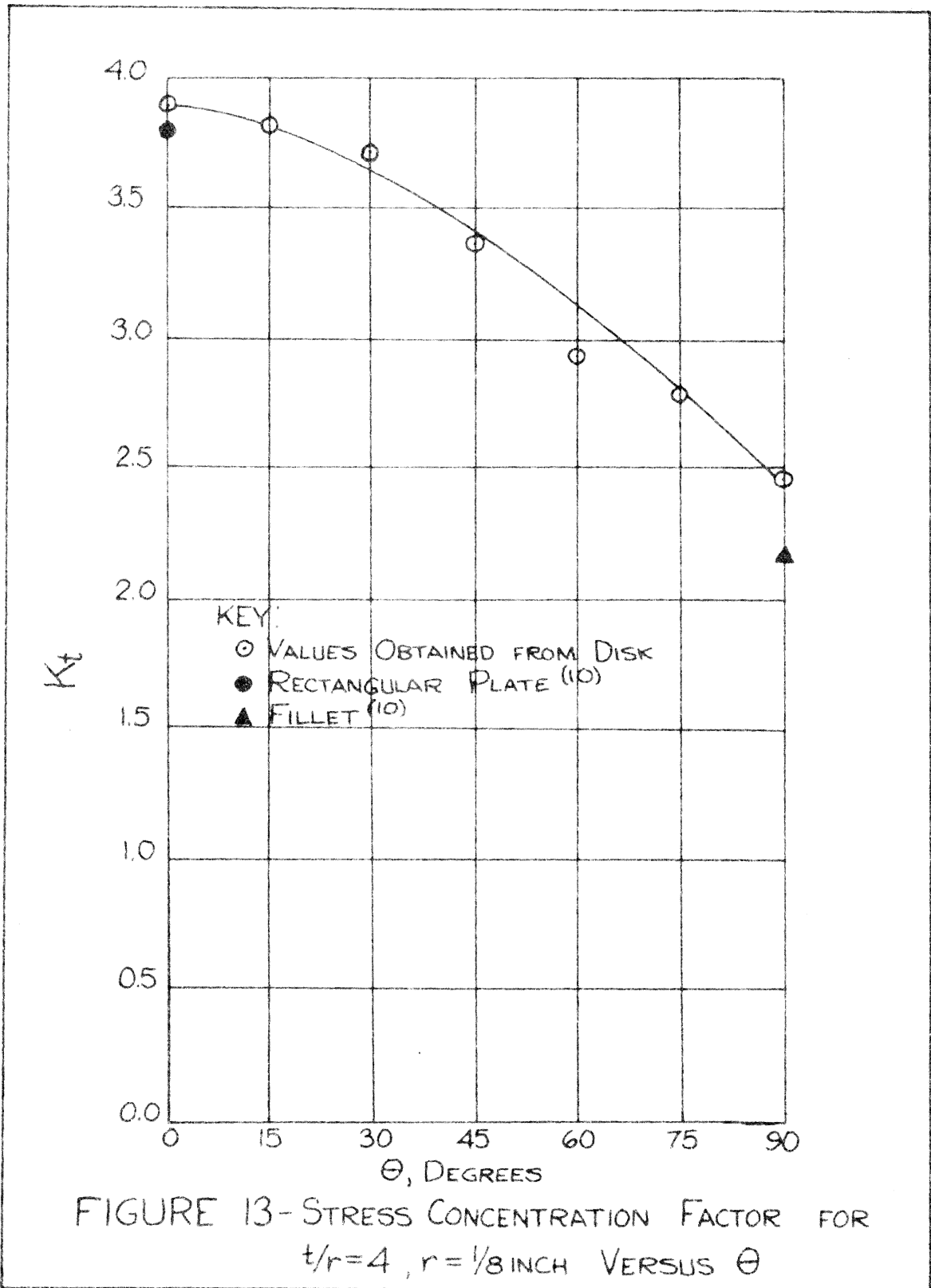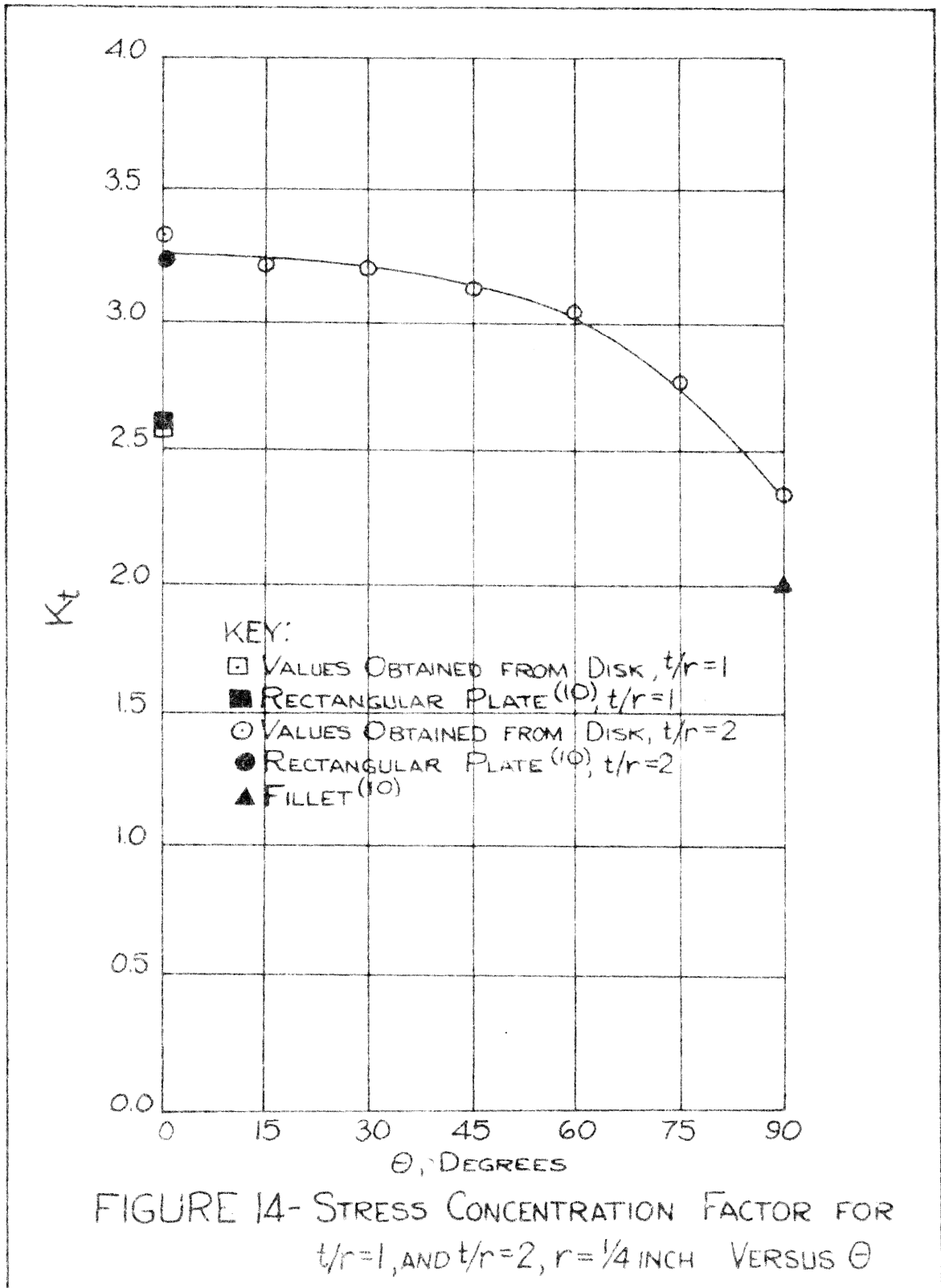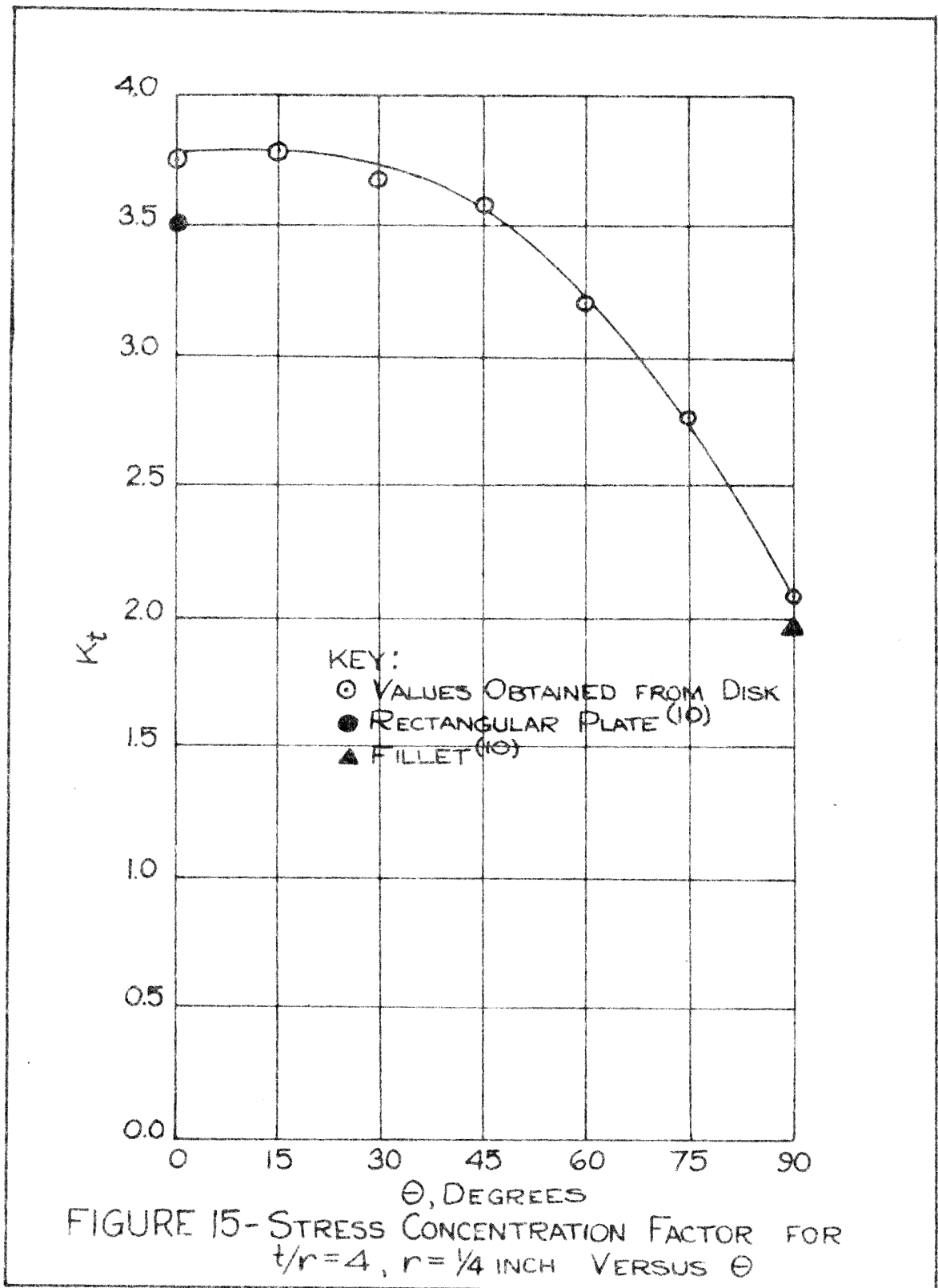FIGURE 15- STRESS CONCENTRATION FACTOR FOR
t/r=4, r=¼ INCH VERSUS Θ

VI. DISCUSSION OF RESULTS

6.1 METHOD OF LOADING

For the method of loading the disk to be satisfactory, it must not only create a uniaxial tension field over the majority of the disk, but should also yield acceptable results for the stress concentrations calculated as compared to the stress concentrations of a similar rectangular plate.

6.1.1 For the stress distribution presented in FIGURE 11 it was evident that the majority of the disk was subject to an approximately uniform tension field next to the grips.

From the comparison of the value of 2.08 for the stress concentration factor of the slot t/r equals four, θ equals ninety degrees, and r equals one-fourth inch against 1.96 for a fillet of the same dimensions, it was seen that good agreement was still obtained. This particular slot was the longest investigated (two inches) and each end came within one-fourth of an inch of the grips. This same slot for θ equals zero degrees yielded a value for the stress concentration factor of 3.73, whereas the value obtained by Frocht was 3.48, which resulted in a difference of 7.2 per cent. Therefore, it appears that this might well be the maximum width and maximum height of the disk that can be used without encountering appreciable error.

6.1.2 From the experience of using this method to create a uniaxial tension field, it was determined that the method was easily reproducible.

From the series of slots investigated, it was a simple procedure to change the direction of the tension field to allow several investigations from one model.

6.2 THE METHOD OF STRESS CONCENTRATION DETERMINATION

The method of stress concentration determination yielded acceptable results when compared with published results.[10] Since two methods, a circular disk used as a rectangular plate and a slope of a load fringe curve for stress concentration factor determination, were being investigated at the same time, it was difficult to determine which errors were attributed to the plate not having a straight boundary and which errors were inherent in the method of stress concentration factor determination. In order to observe the error due to the method alone, three other tests were performed. These three tests were performed on the same disks as before with the modification of machining the sides of the disk straight, so that these results were directly comparable with the known values of stress concentration factors for a slot in a uniaxial tension field. Calculated results were presented in Appendix 11.3. The maximum error of 6% occured for the t/r equal 4 and r equal one-eighth inch slot. This error was not surprising, as this slot falls on the steepest portion of the stress concentration curve[10] being the narrowest slot investigated and was thus the most difficult to determine because of the stress gradient. For the largest slot investigated, t/r equals 4, r equals one-fourth inch, the value obtained by the method used in this paper differed 1.6% from the accepted value. It was noted that the second test,

t/r equals 2, r equals one-eighth inch, yielded results within 0.6% of the accepted value. From these three tests of the method, it could be seen that good results were obtained.

VII. CONCLUSIONS

7.1 METHOD OF LOADING

From the results obtained, the following conclusions were reached regarding the method of loading.

7.1.1   The majority of the disk was subject to uniaxial tension.

7.1.2   The method of loading was easily reproducible in a standard testing laboratory.

7.1.3   Rotation of the disk, to change the direction of the stress field relative to the stress raiser placed in the field, was easily accomplished.

7.2 METHOD OF CALCULATING THE STRESS CONCENTRATION FACTOR

The method of recording the load which caused each fringe to appear on the edge of the slot yielded satisfactory results when compared with a rectangular plate.

7.3 STRESS CONCENTRATION FACTORS FOR INCLINED SLOTS

The maximum stress concentration factor occured when the major axis of the slot was perpendicular to the direction of the uniaxial tension field. The minimum value for θ equal to ninety degrees, approached the value of the stress concentration factor for a fillet.

VIII. <u>ACKNOWLEDGEMENTS</u>

IX BIBLIOGRAPHY

1. Coker, E. G. and Filon, L. N. G.: Photoelasticity, Cambridge at the University Press, 1957.

2. Coolidge, D. J., Jr.: An Investigation of the Mechanical and Stress Optical Properties of Columbia Resin, CR-39, SESA, Vol. VI, No. 1.

3. Edmonds and McMinn: Celluloid as a Medium for Photoelastic Investigation, Trans. ASME, APM 54-8.

4. Frocht, M. M. and Leven, M. M.: Factors of Stress Concentration for Slotted Bars in Tension and Bending, Trans. ASME, Vol. 73 (1951), Applied Mechanics Section, p. 107.

5. Frocht, M. M.: Photoelastic Studies in Stress Concentration, Mech. Engr., Aug. 1936.

6. Frocht, M. M.: Photoelasticity, Vol. 1, John Wiley and Sons, Inc., 1957.

7. Frocht, M. M.: Recent Advances in Photoelasticity, Trans. ASME, Vol. 53 (1931), APM 53-11, pp. 135-153.

8. Hetenyi,: Handbook of Experimental Stress Analysis, John Wiley and Sons, Inc., 1950.

9. Neuber, H.: Theory of Notch Stresses, Edwards Brothers, Inc., Ann Arbor, Mich., 1946.

10. Peterson, R. E.: Stress Concentration Design Factors, John Wiley and Sons, Inc., 1953.

11. Timoshenko, S. and Goodier, J. N.: Theory of Elasticity, McGraw-Hill Book Co., Inc., 1951, pp. 107-109.

12. Wahl, A. M. and Beeuwkes, R., Jr.: <u>Stress Concentration Produced by Holes and Notches</u>, Trans. ASME, Vol. 56 (1934), APM 56-11 pp. 617-625.

The vita has been removed from
the scanned document

XI APPENDIX

11.1 DISCUSSION OF σ_{net}

The accepted definition of σ_{net} for any symmetrical shape is taken to be the load divided by the critical cross-sectional area of the member. This usually corresponds to taking a straight slice through the member at the stress concentration. For the slots considered in this thesis, the straight slice through the member would not give a good indication of the average stress. Since during the rotation of the slot, a symmetry in the stress distribution was maintained, the following definition of σ_{net} was used for the slot.

$$\sigma_{net} = \frac{P}{2Wh} \qquad (11.1.1)$$

Where the quantities are as shown on FIGURE a. below.
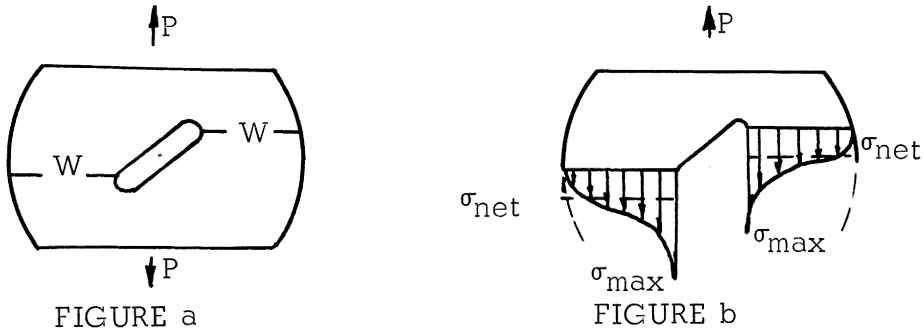
FIGURE a   FIGURE b

From the free-body diagram shown in FIGURE b the symmetry of loading as represented by the stress distribution can be seen. To consider any other section would result in a section not containing σ_{max} or else an unsymmetrical stress distribution.

11. 2 SHEAR DIFFERENCE METHOD APPLIED TO THE DISK

The Shear Difference Method applied across sections A-A, B-B, and C-C, D-D, as shown in FIGURE 6.

Abscissa scale for all curves:

1 Unit = 0. 200 inch

Also 1 unit = distance A-A to B-B and C-C to D-D = 0. 200 in.

FIGURE a – SHEAR DIFFERENCE CURVES ACROSS A-A, B-B

Curves I & II

Curve III
Curve IV
Curve V

FRINGES

UNITS

CURVE I – $\frac{p-q}{2}$ FOR A-A
CURVE II – $\frac{p-q}{2}$ FOR B-B
CURVE III – τ_{xy} FOR A-A
CURVE IV – τ_{xy} FOR B-B
CURVE V – $\Delta\tau_{xy}$
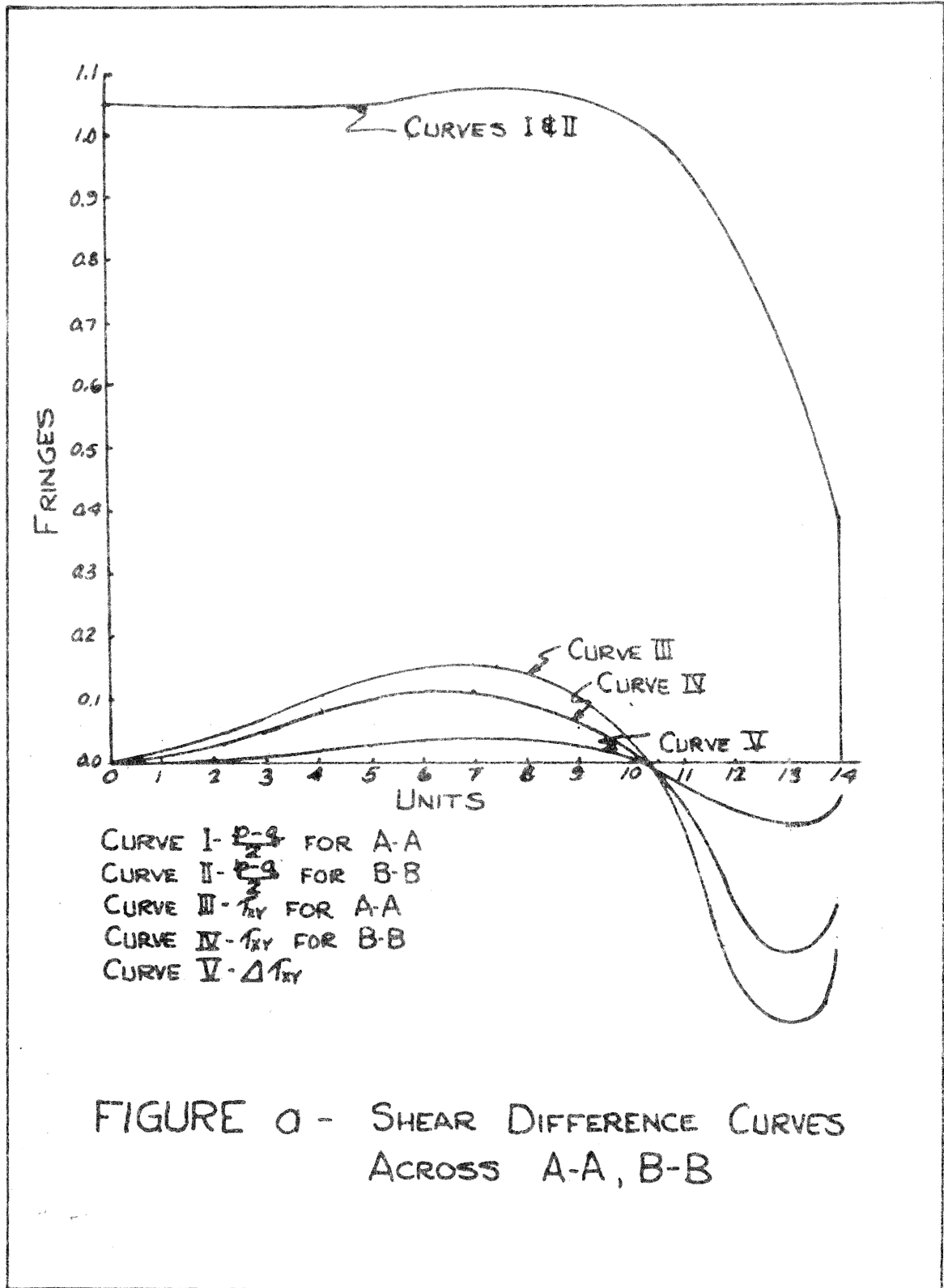
Computation of σ_x, σ_y along A-A, B-B.

STA.	Mean $\Delta \mathcal{M}_{xy} \frac{\Delta X}{\Delta Y}$	σ_x	$p - q$	τ_{XY}	$(p - q)^2$	$4\tau_{XY}^2$	$\sqrt{(p-q)^2 - 4\tau_{XY}^2}$	σ_y
0	0	+0.105	2.10	0	4.42	0	2.10	2.21
1	0.008	+0.097	2.10	0.033	4.42	0.004	2.10	2.20
2	0.030	+0.067	2.10	0.055	4.42	0.012	2.10	2.17
3	0.023	+0.044	2.12	0.082	4.50	0.027	2.11	2.15
4	0.022	+0.022	2.12	0.100	4.50	0.040	2.11	2.13
5	0.029	−0.007	2.14	0.151	4.58	0.091	2.12	2.11
6	0.037	−0.044	2.14	0.131	4.58	0.069	2.12	2.08
7	0.034	−0.078	2.14	0.132	4.58	0.069	2.12	2.04
8	0.037	−0.115	2.12	0.110	4.50	0.048	2.11	1.99
9	0.032	−0.147	2.10	0.075	4.42	0.022	2.10	1.95
10	0.008	−0.155	2.04	0.023	4.17	0.002	2.04	1.88
11	−0.042	−0.113	1.94	0.089	3.77	0.032	1.94	1.83
12	−0.074	−0.039	1.78	0.245	3.17	0.240	1.69	1.65
13	−0.112	+0.073	1.46	0.352	2.13	0.495	1.28	1.35
14	−0.054	+0.137	0.80	0.251	0.64	0.253	0.63	0.77
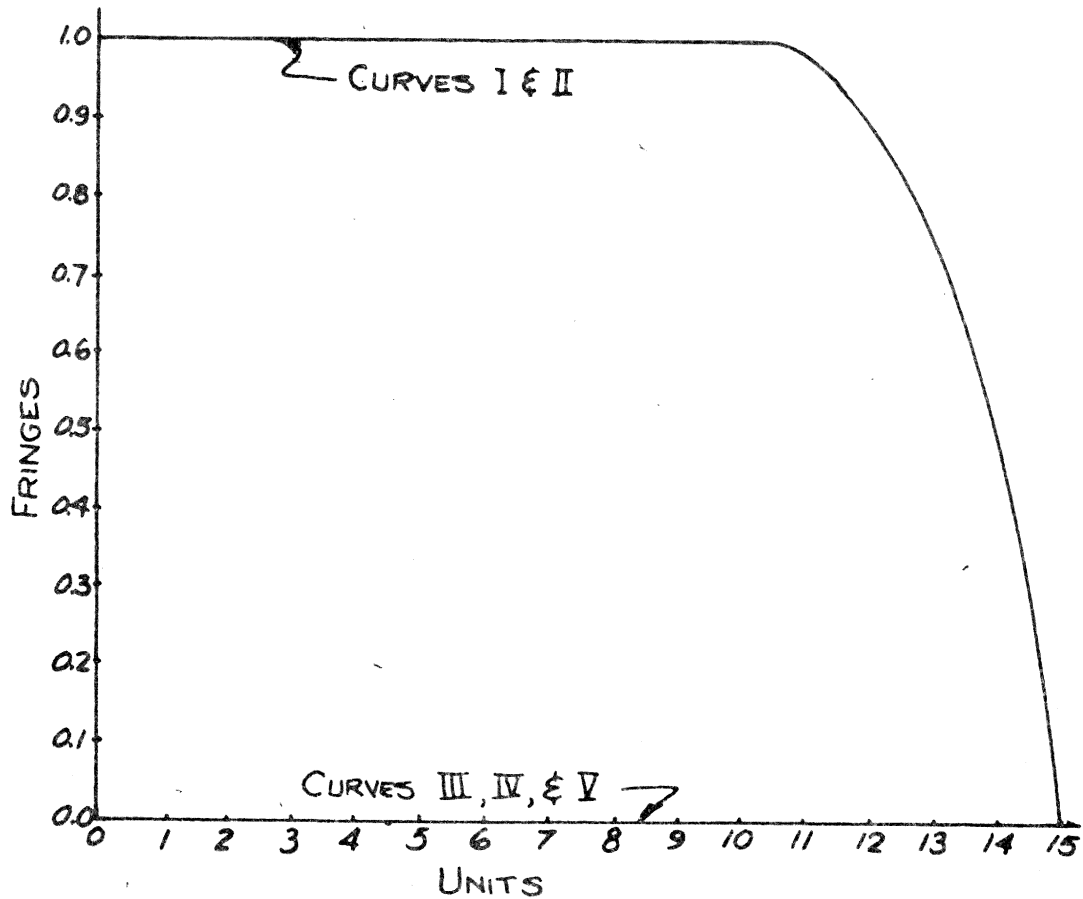
FIGURE b - SHEAR DIFFERENCE CURVES
ACROSS C-C, D-D

Computation σ_x, σ_y along C-C, B-B.

STA.	Mean $\Delta\tau_{xy}\frac{\Delta X}{\Delta Y}$	σ_x	p - q	τ_{xy}	$(p-q)^2$	$4\tau_{xy}^2$	$\sqrt{(p-q)^2-4\tau_{xy}^2}$	σ_y
0	0	0	2.00	0	4.00	0	4.00	2.00
1	0	0	2.00	0	4.00	0	4.00	2.00
2	0	0	2.00	0	4.00	0	4.00	2.00
3	0	0	2.00	0	4.00	0	4.00	2.00
4	0	0	2.00	0	4.00	0	4.00	2.00
5	0	0	2.00	0	4.00	0	4.00	2.00
6	0	0	2.00	0	4.00	0	4.00	2.00
7	0	0	2.00	0	4.00	0	4.00	2.00
8	0	0	2.00	0	4.00	0	4.00	2.00
9	0	0	2.00	0	4.00	0	4.00	2.00
10	0	0	2.00	0	4.00	0	4.00	2.00
11	0	0	1.98	0	3.92	0	3.92	1.98
12	0	0	1.82	0	3.31	0	3.31	1.82
13	0	0	1.50	0	2.25	0	2.25	1.50
14	0	0	0.94	0	0.88	0	0.88	0.94
15	0	0	0.00	0	0.00	0	0.00	0.00

11.3 RECTANGULAR PLATE COMPARISON TESTS

Three rectangular plates were investigated to determine the error inherent in the method. These results are compared to known values,[10] and any error was attributed to the method. The quantities expressing the dimensions of the plate are shown below.
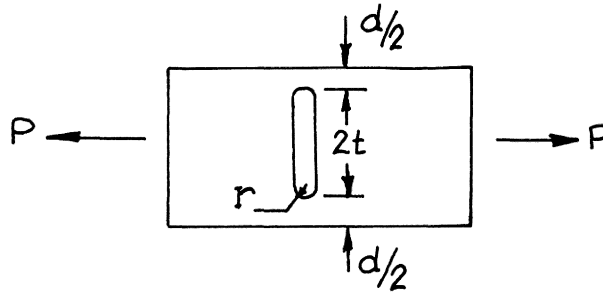
PLATE NUMBER 1 $t/r = 4$, $r = 1/4$ inch, $r/d = 0.233$

LOADING FORCE P, UNITS							
UP	ΔUP	DOWN	ΔDOWN	UP	ΔUP	DOWN	ΔDOWN
492	---	497	30	492	---	497	28
462	30	467	30	462	30	469	29
431	31	437	30	433	29	440	31
403	28	407	---	404	29	409	---

$$\text{Slope} = \Delta_{ave.} = 29.6$$

$$K_1 = \frac{70(1.075)}{29.6} = \underline{2.54} \qquad K_1^{(10)} = 2.58$$

$$\% \text{ Error} = \underline{1.6\%}$$

PLATE NUMBER 2 $t/r = 2$, $r = 1/8$ inch, $r/d = 0.0445$

LOADING FORCE P, UNITS							
UP	ΔUP	DOWN	ΔDOWN	UP	ΔUP	DOWN	ΔDOWN
471	---	484	55	479	---	486	55
412	30	429	57	427	52	431	65

349	63	372	64	363	64	366	58
283	66	308	----	303	60	308	----

$$\text{Slope} = \Delta_{ave.} = 59.8$$

$$K_2 = \frac{70(2.813)}{59.8} = \underline{3.29} \qquad K_2^{(\text{Frocht})} = 3.27$$

$$\% \text{ Error} = \underline{0.6\%}$$

PLATE NUMBER 3 $t/r = 4$, $r = 1/8$, $r/d = 0.054$

LOADING FORCE P, UNITS							
UP	ΔUP	DOWN	ΔDOWN	UP	ΔUP	DOWN	ΔDOWN
485	----	486	41	487	----	488	43
443	42	445	44	441	46	445	41
397	46	401	----	396	45	404	----

$$\text{Slope} = \Delta_{ave.} = 43.5$$

$$K_3 = \frac{70(2.32)}{43.5} = \underline{3.73} \qquad K_3^{(\text{Frocht})} = 3.51$$

$$\% \text{ Error} = \underline{6\%}$$

11. 4 DISCUSSION OF THE STRESS CONCENTRATION FOR A SLOT AS COMPARED TO A FILLET

For the slots with their major axis parallel to the field of tension, the stress concentration factors obtained were compared to the stress concentration factors for a fillet. The reason for doing this is as follows. Consider the plate as shown in FIGURE a. If this plate were sliced along line A-A and separated, as shown in FIGURE b, the resulting member w would reasonably resemble a straight member with a fillet on one side. If the plate were wide as compared to the depth of the fillet and the slot is long, such that one fillet has no appreciable affect on the other fillet, the plate could be considered the same, as shown in FIGURE c. For FIGURE c, the value of the stress concentration factors are known.[10]
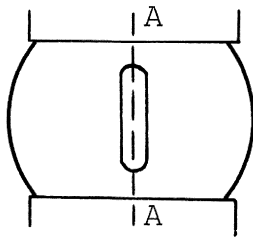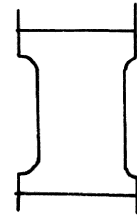
FIGURE a   FIGURE b   FIGURE c

Therefore, for a long slot oriented, as shown in FIGURE a, it would seem that the stress concentration factor should compare closely to that of a fillet. For a short slot the value should lie somewhere between a fillet and a hole. For the two slots investigated, r equals one-eighth inch, and r equals one-fourth inch, these comparisons are shown in FIGURE d.

FIGURE d – Slot – Fillet Comparison
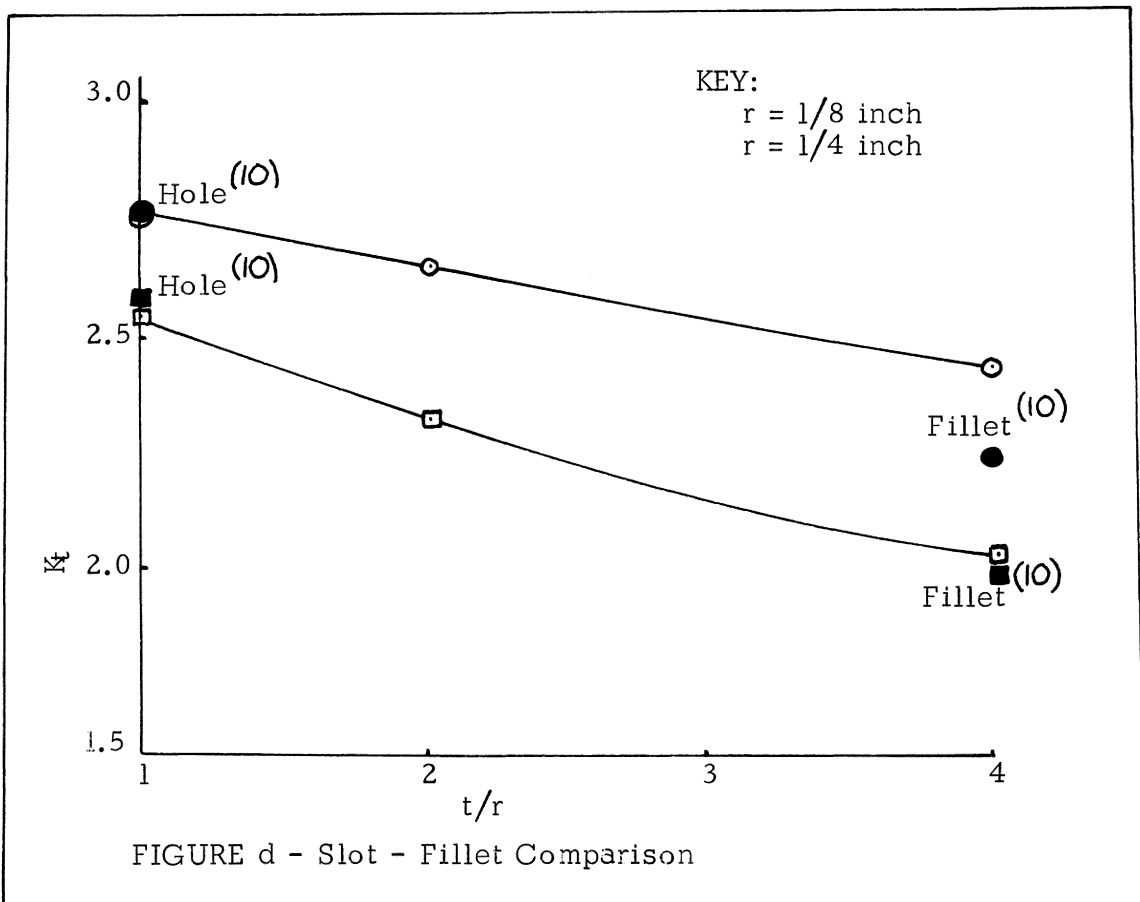
From **FIGURE d**, it can be seen that the assumption of comparing a long slot to a fillet gives good agreement. The greatest deviation occured on the shorter slot as expected.

11. 5 OPTICAL CREEP

The problem of creep occured optically in the following manner.
After the load was applied to produce a fringe at the edge of the hole, it
was noticed that after a period of time the fringe moved farther into the
plate without any further increase in load. Therefore, if the loading was
applied over a long period of time the fringe would increase without any
increase in load. This optical creep property is shown in FIGURE 11.
From FIGURE 11, it can be seen that after ten minutes, the material does
not creep appreciably for small increases in time.

There were thus two different manners of applying the load as to
minimize the error due to optical creep. The first method would be to
increase the load slowly until a fringe appeared at the edge of the hole.
Then allow at least ten minutes to elapse, while making minor adjust-
ments of the load, such that the fringe remained on the edge of the hole.
This process should be repeated for each additional fringe. Then from
curves similar to FIGURE 16, knowing the time of load application and
the fringe value, the desired load-fringe slope could be obtained. The
second method consisted of applying the load rapidly to minimize the
creep. It was found experimentally that to load the disk through a load-
ing cycle of up to four fringes and releasing the load while recording
the corresponding loads when each fringe appeared on the edge of the
slot took three minutes and eight seconds. Therefore, making use of the
relative retardation equation, from Filon and Jessop. [1]

$$r = r_o + pt^{1/3} + qt$$
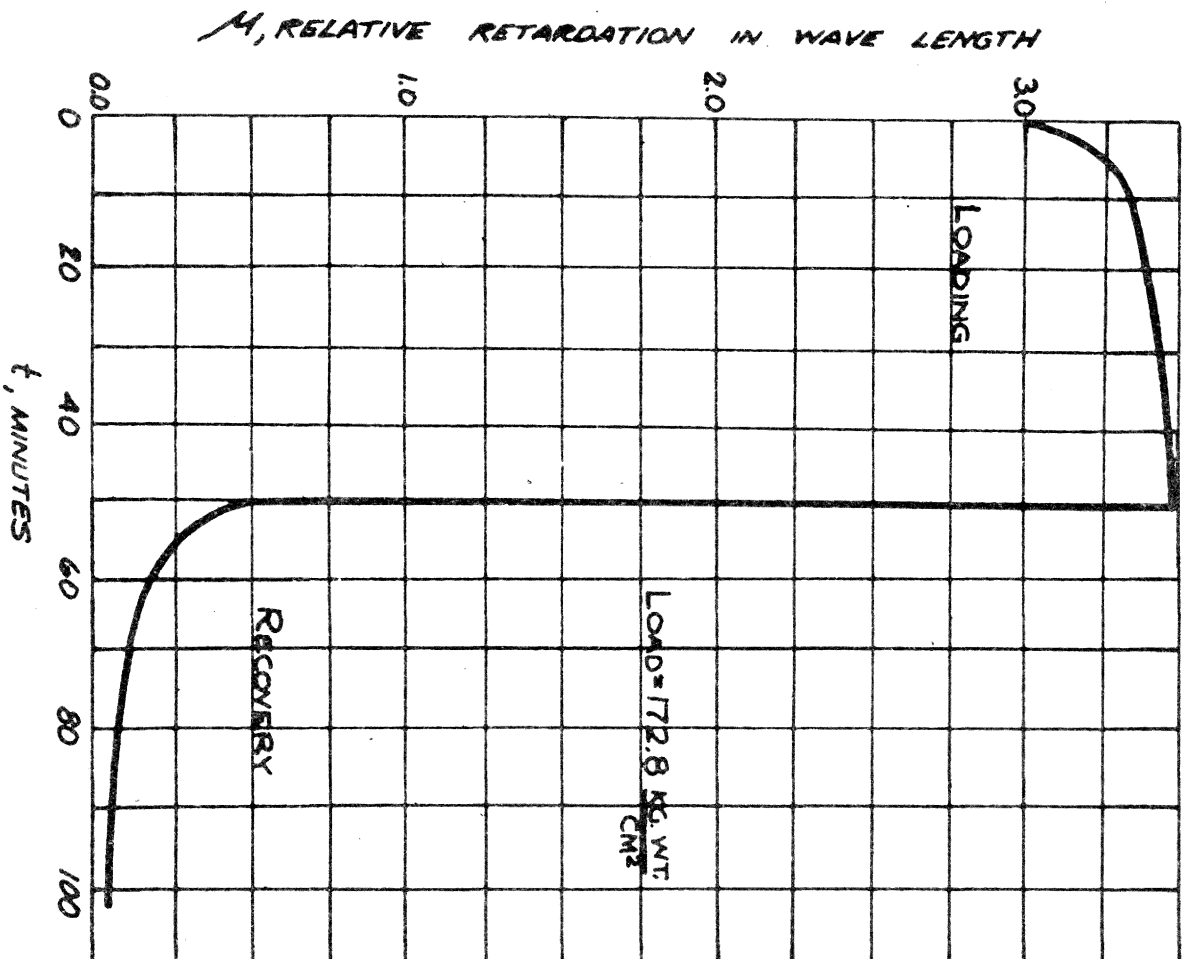
FIGURE a - Optical Creep Curve for C.S.I.(1)

where:

r = The relative retardation at time t.

r_o = The relative retardation at time t = 0.

p, q = Constants

t = Time.

In the above, q is a small constant and since this equation will be used for small periods of time, the third term will be neglected. To evaluate the constant p, data were obtained from "An Investigation of the Mechanical and Stress Optical Properties of Columbia Resin, CR-39" by D. J. Coolidge, Jr.[2]

As an example, consider the fourth fringe at time equal to zero:

$$4 = r_o + p(0) \ 1/3$$

therefore: $\quad r = 4 + pt \ 1/3$

at t= 15 minutes $\quad r = 4.452$

therefore: $\quad 4.452 = 4 + p15 \ 1/3$

solving: $\quad p = 0.183$

As a check, for t = 30 minutes, r = 4.563 and solving:

$$p = 0.181$$

use: $\quad p = 0.182$

But for this investigation the time required to reach four fringes was:

$$t = \frac{3.133}{2} = 1.566 \text{ minutes}$$

therefore: $\quad r = 4 + 0.182(1.566) \ 1/3 = 4.21$

This is considering the maximum creep rate at the fourth fringe as being applied during the upward loading cycle. Even so, this amounts to only 5.3% difference between this reading and the fourth fringe. Since lower loads were actually used in the investigation and since 5.3% is the worst possible creep error, the correction for creep was neglected.

11. 6 SAMPLE CALCULATION

All stress concentration factors were calculated using Equation 5. 3. 6:

$$K_t = \frac{W_m(P_t/n_t)}{W_t(P_m/n_m)}.$$

The quantity:

$$\frac{(P_t/n_t)}{W_t} = 70.0 \frac{units}{inch}$$

was found from a simple tension test. Where one unit equals 1. 22 pounds. Since all loads were measured in these same units, it was not necessary to convert the reading to pounds.

From TABLE 1 the value of:

$$(P_m/n_m) = slope$$

was found by taking the arithmetic average of the differences between any two consecutive readings, W_m was measured with a scale. As an example of the procedure involved to calculate a stress concentration factor, consider the readings for t/r equals one and r equals one-fourth inch. The slope equals 149, and W_m equals 5. 50.

Therefore:

$$K_t = \frac{(70)(5.50)}{149} = 2.58.$$

TABLE 1

EXPERIMENTAL DATA FOR SLOTS

	LOAD IN UNITS						SLOT DIMENSIONS				
FRINGE	UP	DOWN	UP	DOWN	UP	DOWN	θ	SLOPE	t/r	r	WIDTH
1	469	488	482	492	492	498	0		1	1/8	5.75
2	328	322	334	342	340	347					
3	187	191	196	196	203	194		146			
1	420	430	432	432	428	444	0		2	1/8	5.50
2	317	318	321	327	324	337					
3	211	214	211	221	216	234		107			
1	427	435	424	446	425	444	15		2	1/8	5.52
2	315	327	321	335	321	337					
3	206	217	212	224	211	221		109			
1	414	449	416	435	433	441	30		2	1/8	5.54
2	302	328	306	329	326	336					
3	197	212	195	210	206	223		112			
1	432	457	450	451	444	453	45		2	1/8	5.58
2	312	342	330	343	322	341					
3	196	218	215	232	209	222		116			
1	426	430	415	437	423	426	60		2	1/8	5.62
2	295	319	305	322	291	314					
3	185	205	180	200	188	191		117			
1	387	410	407	403	407	410	75		2	1/8	5.67
2	250	262	277	281	271	276		135			

FRINGE	UP	DOWN	UP	DOWN	UP	DOWN	θ	SLOPE	t/r	r	WIDTH
1	500	---	---	---	---	---	90		2	1/8	5.72
2	359	360	371	361	361	351					
3	185	201	214	220	208	215					
1	349	352	351	353							
2	190	215	209	216				149			
1	---	535	570	574	577	580	0		4	1/8	5.00
2	459	448	480	489	484	492					
3	376	363	384	393	386	397					
4	282	285	307	301	297	297		90			
1	549	554	558	569	556	561	15		4	1/8	5.02
2	442	459	462	474	460	467					
3	353	368	373	381	364	375					
4	263	278	283	289	283	286		92			
1	---	563	569	566	565	569	30		4	1/8	5.04
2	425	460	462	472	469	469					
3	343	362	369	369	367	365					
4	253	255	278	277	284	284		95			
1	552	558	546	536	543	558	45		4	1/8	5.10
2	453	452	433	447	443	450					
3	338	342	323	332	338	336					
4	241	243	226	232	224	230		106			
1	550	555	553	551	554	555	60		4	1/8	5.24
2	425	428	429	415	412	423					
3	307	311	303	308	286	303		125			
1	552	517	524	526	525	526	75		4	1/8	5.36
2	384	380	378	381	381	381					
3	259	263	245	249	262	270		135			

FRINGE	UP	DOWN	UP	DOWN	UP	DOWN	θ	SLOPE	t/r	r	WIDTH
1	565	574	573	576	573	575	90		4	1/8	5.66
2	415	410	437	425	405	407					
3	250	252	259	262	238	247		161			
1	463	471	461	463	460	462	0		1	1/4	5.50
2	315	319	315	317	304	314					
3	164	167	168	165	163	163		149			
1	----	500	500	----	----	----	0		2	1/4	5.00
2	----	394	391	401	401	408					
3	----	293	283	298	286	297					
4	----	186	188	187	189	186		105			
1	----	488	489	486	485	490	15		2	1/4	5.03
2	----	375	371	377	373	377					
3	----	260	263	268	264	271					
4	----	154	161	161	161	160		109			
1	490	----	500	----	500	----	30		2	1/4	5.07
2	382	399	388	394	388	394					
3	271	284	278	280	277	275					
4	172	175	172	170	173	171		110			
1	469	----	500	----	491	500	45		2	1/4	5.15
2	355	377	369	382	367	380					
3	247	259	257	261	255	257					
4	144	143	150	148	145	142		115			
1	445	478	473	488	479	490	60		2	1/4	5.24
2	334	359	356	360	359	361					
3	219	227	231	232	228	235					
4	111	113	120	116	116	110		120			

FRINGE	UP	DOWN	UP	DOWN	UP	DOWN	θ	SLOPE	t/r	r	WIDTH
1	454	463	461	462	464	467	75		2	1/4	5.34
2	318	317	325	324	322	328					
3	189	185	195	187	193	188		135			
1	440	472	452	475	466	470	90		2	1/4	5.49
2	273	284	292	296	300	296					
3	123	120	136	133	145	140		165			
1	---	432	425	437	430	448	0		4	1/4	4.00
2	---	360	353	364	354	372					
3	---	284	279	284	284	294		75			
1	427	434	432	434			15		4	1/4	4.07
2	348	357	354	362							
3	279	280	281	282				75			
1	418	435	432	434			30		4	1/4	4.17
2	342	353	348	352							
3	266	272	268	273				79			
1	417	425	423	434			45		4	1/4	4.34
2	329	336	339	348							
3	246	---	249	260				87			
1	404	418	416	421			60		4	1/4	4.58
2	311	315	314	320							
3	214	213	214	212				100			
1	370	391	388	390			75		4	1/4	4.90
2	249	268	259	267							
3	136	136	136	137				124			
1	455	482	484	489	487	500	90		4	1/4	5.32

FRINGE	UP	DOWN	UP	DOWN	UP	DOWN	θ	SLOPE	t/r	r	WIDTH
2	284	291	307	294	310	310	90		4	1/4	5.32
3	116	114	133	131	128	127		179			

A SIMPLIFIED METHOD FOR THE PHOTOELASTIC
DETERMINATION OF STRESS CONCENTRATION FACTORS
IN A TENSILE STRESS FIELD

ABSTRACT

The stress concentration factors for rectangular slots with semicircular ends with their major axes inclined to the direction of a uniaxial tension field were investigated by photoelastic methods. A major portion of this thesis deals with the problem of loading a circular disk such as to create an approximately uniform tension field. This circular disk was used to investigate the stress concentration factors of the slots which were compared to the known results of a slot perpendicular to a tension field in a rectangular plate. The maximum value for the stress concentration factor occured when the slot was perpendicular to the direction of the tension field. A method of determining the stress concentration was developed which required only the recording of the load at which each fringe appeared on the edge of the slot. This method gave results within 6% of accepted values.